HHS Public Access

Author manuscript

Gene Ther. Author manuscript; available in PMC 2013 September 01.

Published in final edited form as:

Gene Ther. 2013 March ; 20(3): 328–337. doi:10.1038/gt.2012.46.

Distinct Transduction Difference Between Adeno-Associated Virus Type 1 and Type 6 Vectors in Human Polarized Airway Epithelia

Ziying Yan[1,3], **Diana Chi Man Lei-Butters**[1], **Nicholas W. Keiser**[1], and **John F. Engelhardt**[1,2,3]

[1]Department of Anatomy and Cell Biology, University of Iowa School of Medicine, Iowa City, IA 52242, USA

[2]Department of Internal Medicine, University of Iowa School of Medicine, Iowa City, IA 52242, USA

[3]Center for Gene Therapy, University of Iowa School of Medicine, Iowa City, IA 52242, USA

Abstract

Of the many biologically isolated AAV serotypes, AAV1 and AAV6 share the highest degree of sequence homology, with only six different capsid residues. We compared the transduction efficiencies of rAAV1 and rAAV6 in primary polarized human airway epithelia (HAE) and found significant differences in their abilities to transduce epithelia from the apical and basolateral membranes. rAAV1 transduction was ~10-fold higher than rAAV6 following apical infection, while rAAV6 transduction was ~10-fold higher than rAAV1 following basolateral infection. Furthermore, rAAV6 demonstrated significant polarity of transduction (100-fold; basolateral≫apical), while rAAV1 transduced from both membranes with equal efficiency. To evaluate capsid residues responsible for the observed serotype differences, we mutated the six divergent amino acids either alone or in combination. Results from these studies demonstrated that capsid residues 418 and 513 most significantly controlled membrane polarity differences in transduction between serotypes, with the rAAV6-D418E/K513E mutant demonstrating decreased (~10-fold) basolateral transduction and the rAAV1-E418D/E513K mutant demonstrating a transduction polarity identical to rAAV6-WT. However, none of the rAAV6 mutants obtained apical transduction efficiencies of rAAV1-WT, suggesting that all six divergent capsid residues in AAV1 act in concert to improve apical transduction of HAE.

Keywords

AAV1 and AAV6; Transduction Polarity; Human Airway Epithelia

Correspond to: John F. Engelhardt, Ph.D., Department of Anatomy and Cell Biology, University of Iowa Department of Anatomy and Cell Biology, Room 1-111 BSB, 51 Newton Road, Iowa City, IA 52242-1109, Tel: 319-335-7753, Fax: 319-335-7198, john-engelhardt@uiowa.edu.

CONFLICT OF INTEREST

The authors declare no conflict of interest.

INTRODUCTION

Adeno-associated virus (AAV) is a nonpathogenic parvovirus with a 4.7kb single-stranded DNA genome[1]. The viral DNA is packaged in a non-enveloped capsid composed of three structural proteins designated as VP1, VP2 and VP3, in a ratio of 1:1:10. These proteins are encoded in the same primary RNA transcript from the p40 promoter and are translated through alternative RNA splicing or alternative start codons. Since the establishment of the first infectious plasmid clone of the AAV type-2 genome in early 1980s, AAV has been developed as a promising viral vector for human gene therapy[2, 3]. Though the AAV type-2 vector is the most extensively studied serotype, numerous AAV serotypes and variants have been isolated from human/non-human primate samples and characterized to have variable tissue tropisms[4–6]. More recent, novel AAV variants have also been engineered through capsid domain-swapping between different serotypes or DNA shuffling combined with directed evolution[7–9]. Vectors based on various AAV serotypes and variants distinguish themselves in their cell-type/tissue tropisms and susceptibility to neutralization antibodies, thus expanding the AAV vector toolbox and flexibility for AAV applications in human gene therapy[5, 10].

Although the specific cell-type/tissue tropisms of certain AAV serotype/variant vectors have been well reported, the mechanism(s) underlying the AAV serotype/variant tropisms remains largely unclear. It is generally thought that interactions between the virion and target cell affect tropism and can occur at the stage of virus binding, entry, intracellular trafficking, and uncoating. It is obvious that the differences in capsid protein coding sequence control divergent tissue tropisms and serological properties, as the AAV capsid is the primary interface with the cell that defines the transduction biology. Comparison of the capsid amino acid sequences of AAV type 1 to 9 demonstrated that the variability between the serotypes is not evenly distributed, but rather concentrated in looped domains that are displayed on the virion surface, while the amino acid residues at N- and C- termini are relatively conserved[11]. More interestingly, transgene expression studies from the AAV variants obtained from directed evolution reveal that virus/host interaction appear to be controlled by a limited number of amino-acid residues—subtle mutations or exchange of certain amino-acids on the capsid surface significantly altering transduction efficiencies between the AAV variant vectors[9, 12].

Of the biologically isolated and defined AAV serotypes, the AAV1 and AAV6 share the highest degree of sequence homology, differing in only six capsid amino acid residues. Despite the high sequence homology and extremely similar serological profiles of AAV1 and AAV6, AAV6 displays a unique heparan sulfate proteoglycan binding characteristic, despite the fact the addition of heparin does not inhibit AAV6 transduction[13, 14]. It was reported that the AAV1 and AAV6 both utilize the α-2,3 and α-2,6 N-linked sialic acids as the primary binding receptors for transduction, and interestingly, AAV6 is more dependent on sialic acid or sialic acid-containing glycoprotein than AAV1 for cell entry and/or the subsequent steps of infection of hepatocytes[15]. Side by side transduction comparison of AAV1 and AAV6 vectors in mouse liver demonstrated that AAV6 delivered consistently higher transgene expression with faster kinetics than AAV1[16]. Differences in the levels and kinetics of transgene expression between AAV1 and AAV6 vectors were also observed in

various cultured cell lines including that derived from human liver cells[17]. These facts suggested that the six amino acid residue differences between AAV1 and AAV6 control disparities in transduction biology between the two serotypes.

AAV-mediated gene therapy for cystic fibrosis (CF) has been hampered by the low efficiencies of AAV transduction in the airway[3, 18]. An AAV2-based vector was the first serotype used for the gene therapy clinical trials to deliver the normal cystic fibrosis transmembrane regulator (*CFTR*) gene to the lungs of CF patients. The phase I and II trials for CF lung disease with rAAV2 have demonstrated a promising vector safety profile; however, these trials were not successful at correcting the CF pulmonary phenotype[19–21]. rAAV2-mediated *CFTR* gene expression in these trials was below the levels needed to detect transgene-derived *CFTR* mRNA, despite the persistence of substantial rAAV DNA viral genomes in the airway epithelia[19–21]. These studies and others[22] suggest that post-entry barriers and impaired intracellular processing of rAAV2 are primarily responsible for low level transduction from the apical surface of human airway epithelia (HAE). However, rAAV2 transduces the basolateral surface of human airway epithelia (HAE) 200-fold greater than the apical surface due to altered endosomal processing[22]. Interestingly, rAAV2/1 does not retain this polarity bias and equally transduces HAE from both membranes[23]. Whether rAAV6 maintains differences in apical and basolateral transduction of HAE remains unknown. Subsequent studies revealed that the ubiquitin/proteasome pathway controls intracellular processing of AAV2 and other AAV serotypes[24–26], and that inefficient endosomal processing or/and nuclear transport in polarized airway epithelia could be overcome by the addition of proteasome inhibitors[22, 23, 27]. Although proteasome inhibitor treatment may eventually be an effective adjunct method to enhance rAAV2-mediated gene delivery for CF lung disease, alternative AAV vectors that are less susceptible to ubiquitin/proteasome blocks and/or other trafficking barriers would be a better choice to improve current clinical trials for CF.

The levels of transgene expression following apical infection of polarized human airway epithelia with rAAV1 and rAAV6 has been suggested to be substantially higher than that of AAV2[23, 28]. These two serotypes also demonstrate improved gene transfer efficiency in the airway of experimental animals including mouse, rabbit, dog and chimpanzee[13, 29–31]. More recently, AAV variants with enhanced apical transduction were successfully generated from capsid-directed evolution on polarized HAE culture. Of those variants evolved from the chimeric AAV capsid library generated by DNA shuffling from eight AAV serotypes, one of the best performing vectors was the chimera of AAV1 and AAV6 capsids, whereas another was the chimera of AAV1, AAV6, and AAV9, with its major capsid component VP3 derived from AAV1 and AAV6[12].

It remains unclear what capsid features of AAV1 and 6 make them potentially attractive vectors for gene therapy to the airway. It has been reported that rAAV6 transduces polarized HAE ~2-fold more efficiently than AAV1[28]. In addition, an AAV6 mutant (AAV6.2) with a single amino acid residue exchange at the position 129 in the VP1 protein, mutating the phenylalanine residue (AAV6) to leucine (AAV1), resulted in increased (~2-fold) airway transgene expression over its parental AAV6 vector[28]. However, in the studies evaluating HAE transduction, extremely high titers of virus were used for infection (10^{11} particles per

well or MOI=100,000 particles/cell with an estimation about 10^6 cells per MilliCell insert). Because the MOI has been suggested to impact intracellular tracking of AAV[32], we sought to make similar comparisons between rAAV1 and rAAV6 transduction of HAE at 20-fold lower titers of infection, a dose we reasoned might be more relevant to *in vivo* studies in humans. During the course of these studies, we observed several interesting features about rAAV1 and rAAV6 transduction biology of HAE not previously reported. First, using viral preparations purified by identical methods and proviral plasmids, we observe that apical infection of HAE with rAAV1 leads to 10-fold greater transduction than rAAV6. Second, rAAV6 retains an interesting polarity bias not observed with rAAV1; rAAV6 transduced the basolateral membrane of HAE ~100-fold more effectively than the apical membrane, while rAAV1 transduced HAE equally well from both the apical and basolateral membranes. Lastly, capsid amino acid differences between rAAV6 and rAAV1 that control unique properties of apical and basolateral transduction of HAE were identified by mutation analysis. We conclude that all six amino acids in rAAV1 that are different from rAAV6 act in concert to enhance apical transduction of HAE by rAAV1, while differences in the polarity of transduction between rAAV6 and rAAV1 is dependent on capsid residues 418 and 531. In this context, the rAAV1-E418D/E531K mutant had HAE transduction biology identical to rAAV6-WT. In contrast to a previous report[28], our studies revealed that the F129L-rAAV6 mutant (i.e., rAAV6.2) was less effective at transducing HAE than the parental rAAV6 virus. Furthermore, we demonstrate that the rAAV6 transduction of HAE from the apical surface is extremely sensitive to the resistance of the epithelium, with lower resistance epithelia having significantly higher transduction efficiencies following apical delivery of the virus. Thus, the extent of polarization of HAE can significantly influence rAAV6 transduction biology, likely through redistribution of AAV6 receptors to the apical membrane or leakage of virus to the basolateral side of the epithelium. These studies suggest that rAAV1 may be the preferred vector serotype compared to rAAV6 for CF lung gene therapy.

RESULTS

Transduction efficiencies of rAAV1 and rAAV6 in HeLa cells and IB3 cells

Since the goal of these studies was to compare differences in apical and basolateral transduction of human airway epithelia by rAAV1 and rAAV6, it was important to demonstrate that these viruses, when purified by the same method, and using the same proviral vector backbones, had similar functional potential to express an encoded transgene. Assessment of vector functionality was performed in two cell lines that are highly susceptible to infection by both serotypes (HeLa and IB3 cells). To our knowledge, such a direct comparison between these two serotypes has not been previously performed using similar packaging systems. To this end, we generated identical packaging systems by cloning the region of capsid difference in AAV6 into a common rAAV2/1 packaging plasmid and generated virus (rAAV2/6 and rAAV2/1) with an identical procedure using CsCl banding, followed by sucrose step cushion ultracentrifugation to remove impurities. Both serotypes generated similar titers and purity by SDS-PAGE (Figure 1a) and very few empty particles were observed by electron microscopy (Figure 1b). The two cell lines were infected with equal amounts of AAV2/1-Luc or AAV2/6-Luc (multiplicity of infection

[MOI] = 5000 DNase resistant particles [DRP] per cell), uptake of viral genomes was evaluated at 2 and 24 hrs post-infection, and luciferase transgene expression was evaluated at 24 hrs post-infection. In HeLa cells, these two serotypes demonstrated very similar viral genome uptake and transduction profiles (Figure 1c and 1d). Using a human airway epithelial cell line (IB3), rAAV6 appeared to be more rapidly taken up, as indicated by greater cell-associated viral genomes by 2 hrs post-infection, and this was also reflected by higher transduction with rAAV6, as compared to rAAV1, by 24 hrs (Figure 1e and 1f). These studies demonstrated that the rAAV1 and rAAV6 viruses have similar function in HeLa cells, and that rAAV6 is slightly more effective in IB3 cells. We conclude that these recombinant viruses are suitable for evaluating differences in transduction biology of polarized human airway epithelia.

AAV1 and AAV6 vectors demonstrate differences in the polarity of transduction of human polarized airway epithelia

To investigate whether rAAV2/1 and rAAV2/6 infect HAE in a similar fashion from both membranes, ALI cultures were infected with rAAV-Luc (MOI = 5000 DRP/cell) for 16 hrs, and luciferase transgene expression continually monitored by biophotonic imaging over a 14-day period. Results from two representative experiments on independent donor-derived HAE are shown in Figure 2a and 2b. Consistent with our previous observations[23], rAAV2/1 lacked a transduction polarity bias, with the time courses of transgene expression following apical and basal infections demonstrating identical patterns. By contrast, rAAV2/6 demonstrated a significant difference in transduction polarity, with over two orders of magnitude greater transduction from the basolateral membrane as compared to the apical membrane. Notably, rAAV2/1 transduced HAE from the apical surface ~10-fold more efficiently than rAAV2/6, while the basolateral transduction of rAAV2/6 produced >10-fold higher levels of transgene expression as compared to both apical or basolateral infection by rAAV2/1. Given the differences observed here in comparison to those previously reported for rAAV1 and rAAV6 apical transduction of HAE (rAAV6 > rAAV1 by ~2-fold)[28], the differences in basolateral transduction between these serotypes is noteworthy.

Other notable features of HAE infection with these two serotypes included differences in the kinetics of transduction. Basolateral infection by rAAV2/6 produced the most rapid rise in transgene expression, reaching its peak by nearly 2 days post-infection. By stark contrast, apical infection with AAV2/6 led to a much slower rise in transgene expression, with a 13-fold increase over the 2-week test period. In the case of rAAV2/1 infections, no differences in the transgene expression kinetics were observed following apical and basal infections. However, rAAV2/1 apical and basolateral infection demonstrated a slow gradual rise in transgene expression between 2–14 days post-infection, with the greatest increase between day 1 and 2.

Combined analysis of eight independent donor-derived ALI cultures using 3–4 independent viral preparations for each serotype demonstrated similarly divergent transduction polarity between these two close serotypes (Figure 2c and Table 1) and higher levels of apical transduction with rAAV2/1 than with rAAV2/6 (Figure 2d and Table 2). For this analysis, we calculated the transduction polarity for each experiment and donor sample by evaluating

the ratio of luciferase expression following basolateral and apical infection (Table 1). Although there was variation in this polarity index between donor samples, the trends demonstrated a clear polarity bias (basolateral > apical) for rAAV2/6, but not rAAV2/1, with a range in the ratio of basolateral/apical luciferase expression from 0.22 to 2.19 for rAAV2/1 and 54 to 445 for rAAV2/6 (Table 1). Figure 2c depicts the average results from these experiments, which resulted in basolateral/apical transduction ratios of 0.81+/−0.16 for rAAV2/1 and 176+/−48 for rAAV2/6. The higher apical transduction efficiency of rAAV2/1, in comparison to rAAV2/6, was confirmed in analysis of multiple donors at 3- and 7-day post-infection time points (Figure 2d and Table 2). Figure 2d shows the average fold difference in apical transduction efficiencies of rAAV1 relative to rAAV6 (normalized to 1 for each experiment) from side-by-side comparisons using multiple donor tissues (the individual data are summarized in Table 2). These studies demonstrate that the transgene expression following apical infection with rAAV1 is more than 10-fold higher than that with rAAV6.

Post-entry processing differences are the major cause of divergent apical transduction of HAE by rAAV1 and rAAV6

Although it remains unclear what receptors rAAV1 or rAAV6 utilize to infect polarized airway epithelia, we hypothesized that the divergent apical (rAAV2/1 > rAAV2/6; ~10-fold) and basolateral (rAAV2/6 > rAAV2/1; ~100-fold) transduction efficiencies by these two serotypes was due to differences in viral uptake from each of the membranes. To the end, we quantified internalized viral genomes using quantitative real-time PCR and luciferase transgene expression at 18 hours and 3 days post-infection (Figure 3a). Analysis for rAAV2/1 demonstrated that 18.3- and 14.6-fold less rAAV1 viral genomes were taken up by the basolateral membrane at 18 hrs and 3 days, as compared to the apical membrane, despite similar levels of transduction from both membranes (Figure 3b and Figure 2c). Comparison of the viral efficiencies (transgene expression/viral genome) (Figure 3c) suggests that the endocytosed rAAV2/1 virions are processed more efficiently from the basolateral membrane, and implicates different infection pathways from the two membranes. In contrast to rAAV2/1, analysis of rAAV2/6 demonstrated that viral uptake was significantly more efficient from the basolateral membrane (11.1-fold at 18 hrs and 6.5-fold at 3 days) (Figure 3a). However, the greater number of virions taken up from that basolateral membrane did not completely account for the significantly higher efficiency of basolateral transduction (1632-fold at 18 hrs and 238-fold at 3 days) (Figure 3a and b). Indeed, like rAAV2/1, viral processing pathways of rAAV2/6 was significantly more efficient from the basolateral than from the apical membrane, based on the transgene expression/viral genome ratios at 18 hr and 3 days post-infection (Figure 3c). This suggests that both more efficient viral endocytosis and virion processing control the high levels of basolateral transduction by rAAV2/6. By 3 days post-infection, viral genome efficiency following apical transduction (i.e., transgene expression/viral genome) was significantly higher (3.2-fold) for rAAV2/1 than rAAV2/6, implicating differences in transduction biology from the apical membrane.

Amino acid capsid differences at position 418 and 531 most significantly influence differences in HAE transduction polarity by rAAV1 and rAAV6

We next sought to evaluate which of the six amino acids differences between AAV1 and AAV6 were responsible for the observed differences in transduction of polarized HAE from the apical and basolateral membranes. Alignment of various AAV capsid proteins sequences for different serotypes indicated that the amino acid residues at positions 418 and 642 are located within a structurally conserved region. The remaining four amino acid differences at positions 129, 531, 584, and 598 are located within, or close to, the variable regions (VR) that are important structural determinants for virus transduction or antigenic recognition[11, 33, 34]. Recent structural analysis of AAV1 and AAV6 viral-like-particles (VLP) has revealed that residues 418 and 642 are located on the interior of the virion and residues 531, 584 and 598 on the exterior surface of capsid, while the location of residue 129 remains unknown since the VP1 protein was not included in the VLP[35]. Analysis of available AAV serotype crystal structures demonstrated that the variable regions VRI and VRVI are commonly divergent[11, 33, 35–37]. Although AAV1 and AAV6 exhibit the fewest structural differences, superimposing the crystal structures of AAV1 and AAV6 revealed that they still adopted slightly different conformation in VRVI, where residue 531 is located[35]. To determine which amino acids most significantly influenced the transduction behavior of rAAV1 and rAAV6 in HAE, we constructed six AAV6 capsid mutant luciferase viruses depicted in Figure 4a (rAAV2/6-F129L, rAAV2/6-L584F, rAAV2/6-V598A, rAAV2/6-H642N, rAAV2/6-D418E/K531E, and rAAV2/6-F129L/L584F/V598A/H642N). The rAAV2/6-F129L mutant is the equivalent to AAV6.2 previously reported[28].

The mutations did not significantly impact viral production, with some mutants (rAAV2/6-H642N, rAAV2/6-D418E/K531E, and rAAV2/6-F129L/L584F/V598A/H642N) having ~2-fold higher DRP yields, and other mutants (rAAV2/6-F129L, rAAV2/6-L584F, rAAV2/6-V598A) having 1–2 fold lower DRP yields, in comparison to wild type vectors. We first characterized these vectors in HeLa cells by evaluating transgene expression at 24 hour post-infection with equivalent DRP/cells. Given the fact that the rAAV1 and rAAV6 vectors transduced HeLa cells with equal efficiencies, we did not expect that mutations would alter their transduction efficiencies in this cell line. However, we did observe changes in the transduction efficiency of certain mutants, ranging from 7.6-fold lower to 1.7-fold higher in comparison to rAAV2/6-WT (Figure 4b). Viral uptake for all the mutants was quite similar when viral genomes were quantified at 24 hrs, with relatively small differences of 24–43% in comparison to rAAV2/6-WT (Figure 4c). Mutation V598A had no effect on the infection of rAAV2/6 in terms of both transgene expression and virus uptake. Mutations F129L, L584F, H642N, and D418E/K531E led to a 3.4-to 7.6-fold decrease in the transduction of HeLa cells, however, these decreases in transgene expression were not reflected by a general trend of reduced viral uptake. One mutant, F129L/L584F/V598A/H642N, enhanced transduction 1.7-fold without altering viral uptake in comparison to the WT vector. These analyses in HeLa cells support the hypothesis that small alterations in the rAAV6 capsid can lead to statistically significant changes in transduction through post-entry processing of the virus.

We next evaluated apical and basolateral transduction of polarized HAE with these rAAV2/6 mutants (Figure 5). Given that major differences in the kinetics of transgene expression by rAAV2/1 and rAAV2/6 occur within the first 4 days following infection, we chose to evaluate transgene expression at 7 days post-infection from the apical and basolateral membranes (Figure 5a). Additionally, the transduction polarity of each vector was calculated as the quotient of the basal expression divided by apical expression (Figure 5b). Results from this analysis demonstrated that none of the rAAV2/6 mutants had improved transduction of HAE from the apical membrane in comparison to rAAV2/6-WT. Although we cannot rule out that certain other combination of mutations would improve apical transduction by rAAV2/6, these findings do suggest that multiple capsid differences between the two serotypes act in concert to improve apical transduction of HAE.

Despite the fact that all the rAAV2/6 mutants retained a basolateral transduction preference in HAE, one mutant (D418E/K531E) demonstrated a significant change in the polarity of transduction, making it more similar to rAAV2/1. This rAAV2/6-D418E/K531E virus demonstrated a 10-fold reduction in basolateral transduction as compared to rAAV2/6-WT virus, resulting in a level similar to that of the rAAV2/1 (Figure 5a). However, these mutations had no impact on apical transduction by the mutant. Among the rAAV2/6 mutants tested, rAAV2/6-D418E/K531E demonstrated the greatest change in transduction polarity toward that of rAAV2/1 (Figure 5b). These finding demonstrate that the D418 and K531 residues are biologically important for the high level of basolateral transduction by rAAV2/6.

Another interesting finding was that the mutant AAV6-F129L/L584F/V598A/H642N, in contrast to the single mutation vectors F129L, L584F, V598A or H642N, resulted in no changes in transduction in comparison to the parental AAV2/6-WT vector. This quadruple rAAV2/6 mutant also can also be designated as AAV2/1-E418D/E531K, an AAV1 capsid mutant with only two amino acid changes to AAV6 sequence. From this standpoint, only two changes in the AAV1 capsid conferred significant alterations in the transduction polarity, increasing basolateral transduction ~10-fold and decreasing apical transduction ~10-fold. In light of the fact that apical and basolateral infection with AAV2/6-F129L/L584F/V598A/H642N (or AAV2/1-E418DE531K) also behaved identically to AAV2/6-WT, we conclude that capsid amino acids at the position of 418 and 531 are very important for the divergent transduction polarity between these two closely-related AAV serotypes.

Changes to transepithelial resistance of polarized HAE can significantly alter apical transduction by rAAV6

The reasons for why our studies demonstrate ~10-fold higher apical transduction of HAE with rAAV2/1, as compared to the opposite result in HAE previously reported (rAAV2/6 > rAAV2/1 by ~2-fold)[28], is presently unclear. We hypothesized that differences in how tightly polarized the airway epithelia are could account for significant changes in apical transduction by rAAV2/6, since leakage of virus from the apical to the basolateral surface would be expected to greatly enhance transduction. Alternatively, the extent of polarity could influence diffusion of highly efficient AAV6 basolateral receptors to the apical surface. Both of these hypotheses could also potentially explain why we observed an ~8-fold

range (53 to 446) in the transduction polarity index (basal transduction divided by apical transduction) for rAAV2/6 between tissue donors (table 1).

To test whether the degree of polarity of HAE influences rAAV2/6 transduction from apically applied virus, we performed a series of infections following transient EGTA treatment of the epithelium to disrupt tight junctions and thus polarity to various degrees. In these studies, treatment of HAE with various doses of EGTA led to dose-dependent decline in resistance of the epithelium (Figure 6a). In support of our hypothesis, transient reductions in resistance of the epithelium at the time of infection gave rise to significantly greater rAAV2/6 transduction when virus was applied to the apical surface (Figure 6a and b). Furthermore, the degree of resistance also inversely correlated with the extent of transduction—the lower resistance epithelia gave higher transduction by rAAV2/6 from the apical surface. Interestingly, relatively minor reductions in resistance induced by the lowest concentration of EGTA gave rise to relatively large changes in transduction—an 8% reduction in resistance just prior to infection gave rise to a 4-fold enhancement ($p<0.005$) in apical transduction at 7 days post-infection (Figure 6). At the intermediate dose of EGTA, a 35% reduction in resistance gave rise to a 12-fold enhancement ($p<0.001$) in transduction at 7 days post-infection. Thus, we conclude that the observed variability of rAAV2/6 to transduce HAE from the apical surface is significantly impacted by the degree of polarization of the epithelium.

DISCUSSION

With the isolation of so many new rAAV serotypes, evolved mutants, and chimeras, it has been challenging for the field to determine what rAAV vector is optimal for testing in clinical trials of CF lung disease. Indeed, the intricacies of various airway models, titers of infection, and the methods of viral preparation, can all likely influence the outcomes of comparative testing of rAAV vectors. For example, using the identical model system of polarized airway epithelia, rAAV2/2, 2/1, and 2/5 demonstrate significant differences in the efficiencies of both apical and basolateral transduction of human, mouse, pig, ferret, and non-human primate[23, 28, 38–40]. In all the tested species except for rhesus monkey, rAAV1 delivers 10 to 100-fold higher level of transgene expression than rAAV2/2 and rAAV2/5 following apical infection. *In vivo* evaluation of rAAV2/1 and rAAV2/5 airway transduction in chimpanzee, the closest existing genetic relative to *Homo sapiens*, revealed that the rAAV2/1 was superior to rAAV2/5 with a 20-fold higher efficiency[31]. Although chimpanzee polarized airway cultures could not be tested, this finding suggested that serotype differences in transduction exist even among non-human primate species (chimpanzee rAAV2/1 ≫ rAAV2/2 and rAAV2/5; rhesus monkey rAAV2/2 ≫ rAAV2/1 and rAAV2/5). Because of these species-specific differences, polarized human airway epithelia have become the gold standard for assessing transduction profiles of rAAV serotypes for gene therapy of lung disease.

Gene transfer studies using rAAV6, a very close relative of rAAV1, demonstrate that this serotype efficiently transduces airways from different species included mice and dogs *in vivo*[13, 30, 41]. This is perhaps not surprising given the high efficiency of rAAV1 at transducing airway epithelia of most species. However, several reports have begun to

suggest that differences between rAAV2/1 and rAAV2/6 transduction of mouse hepatocytes[15, 16] and both mouse[41] and human airway epithelia[28], with rAAV2/6 performing better than rAAV2/1. An rAAV6 variant, designated as rAAV6.2, performed even better than its parental rAAV6 wild type vector in mouse lung transduction *in vivo* and also in human polarized airway epithelia *in vitro*[28]. Interestingly, rAAV6.2 contains only one amino acid change (F129L) that alters this amino acid to that found in the AAV1 capsid. Based on this report, the rAAV6 and its variants could be better candidate vectors than rAAV1 for CF lung gene therapy. In the present study, we sought to perform a more in depth analysis of what amino acid differences between the AAV6 and AAV1 capsid determine differences in transduction efficiency of human polarized airway epithelia.

Our studies revealed strikingly different transduction profiles between the rAAV2/1 and rAAV2/6 vectors in human polarized airway epithelia, despite similar transduction profiles in HeLa cells. Previously unanticipated differences in transduction polarity between these serotypes was observed—rAAV2/1 transduced epithelia ~10-fold more efficiently from the apical membrane and ~10-fold less efficiently from the basolateral membrane than rAAV2/6. While rAAV2/1 transduction efficiencies from both apical and basolateral membranes were roughly equivalent, rAAV2/6 transduction from the basolateral membrane was ~100-fold more efficient than apical infection. This polarity of transduction by rAAV2/6 is similar to that of rAAV2/2 and rAAV2/5[22, 23]. These differences in the polarity of transduction by rAAV2/1 and rAAV2/6 support the notion that infectious pathways of these two serotypes in human airway epithelia significantly differ.

Serotype differences in rAAV transduction of apical and basolateral membranes of polarized airway epithelia are most likely influenced by serotype-specific receptors and co-receptors that reside in these two membrane compartment. Our findings suggest that the transmembrane resistance of HAE can significantly influence the polarity of rAAV6 transduction, with lower resistance epithelial giving rise to much higher transduction by rAAV6 from the apical surface (Figure 6). The most likely explanation for this finding is redistribution of highly effective basolateral rAAV6 receptors to the apical surface when resistances are low and thus polarity is compromised. Such findings likely explain discrepancies in the efficiency of rAAV6 and rAAV6.2 to infect the apical surface of HAE between a previous study (rAAV6.2>rAAV2/6 > rAAV2/1)[28] and our current studies (rAAV1≫ rAAV6>rAAV2/6.2 or F129L-rAAV6). It is also likely that variation in the extent of HAE polarization between donor samples also explains the observed ~10-fold range in the transduction polarity index of rAAV2/1 in our studies (table 1; 0.22 to 2.19), since viral processing from the basolateral surface appears to be more efficient for this serotype (i.e., transduction per viral genome taken up by HAE was greater following basolateral infection as compared to the apical infection, Figure 3c).

The different transduction polarities between these two serotypes led us to investigate which of the six amino acids differences between the AAV1 and AAV6 capsids were most important in controlling this divergent biology. The results revealed that two amino acid residues in the AAV6 capsid (D418 and K531) had the most significant influence on basolateral transduction—when these residues were mutated to the AAV1 sequence (D418E and K531E), the basolateral transduction efficiency of the mutant rAAV2/6-D418E/K531E

vector was similar to that of rAAV2/1. This same rAAV2/6-D418E/K531E mutant can also be considered a rAAV2/1-L129F/F584L/A598V/N642H mutant and given its ~10-fold reduced level of apical transduction as compared to rAAV2/1-WT virus, we concluded these amino acids (L129/F584/A598/N642) are important for the higher apical transduction by rAAV2/1. However, mutagenesis of each of these amino acids singly within the AAV6 capsid to the AAV1 sequence failed to restore apical transduction efficiencies to rAAV2/1-WT levels. Additionally, the rAAV2/6-F129L/L584F/V598A/H642V mutant (same as a rAAV2/1-E418D/E513K mutant) retained apical and basolateral transduction profiles identical to rAAV2/6-WT virus, suggesting that E418 and E513 in the rAAV2/1 capsid also play significant roles in apical transduction. Thus, we conclude that the six amino acid differences in the AAV1 capsid act in concert to control its higher level of apical transduction in comparison to AAV6.

Vector genome analyses demonstrated that differences in transgene expression following rAAV2/1 and rAAV2/6 basolateral infection are most-likely related to differing amounts of viral uptake—significantly more viral uptake of rAAV2/6 from the basolateral surface (100- and 23-fold at 18 hr and 3 day time points, respectively) correlated with higher transgene expression. Although differences in viral uptake from the apical surface were less pronounced for the two serotypes (4.5- and 3.2-fold greater for rAAV2/1 at 18 hrs and 3 days post-infection), this most likely contributed to the ~10-fold higher transduction by rAAV2/1. Since capsid amino acid 531 is located on the exterior surface of the AAV1 or AAV6 virions, it is likely E531 or K531 residues are involved in virion binding and uptake. It was reported that the K531 residue in the AAV6 capsid is essential for the heparin binding characteristic of AAV6 and important for the higher transduction of hepatocytes by AAV6 than AAV1[14]; however, competitive binding with heparin has been reported to not affect rAAV6 infection of an immortalized human airway cell line[13]. Thus, it remains unclear if heparan sulfate proteoglycans mediates higher-level basolateral transduction by rAAV6.

In summary, we find that the two very closely related rAAV1 and rAAV6 serotypes have significantly different biologic properties as recombinant viruses when infecting polarized human airway epithelia from the apical and basolateral membranes. AAV6 capsid amino acids F129, L584, V598, and H642 appear to play little role in the significant transduction polarity observed with rAAV2/6 (basolateral ≫ apical). By contrast, capsid amino acids D418 and/or K531 appear to most significantly control enhanced basolateral transduction by rAAV2/6. The enhanced ability of rAAV2/1 to transduce polarize human airway epithelia from the apical membrane appears to require most, if not all, the amino acids that differ with AAV6 capsid. Studies comparing rAAV1 and other serotypes such as rAAV2 and rAAV5 have demonstrated similar viral uptake from the apical and basolateral surfaces of HAE, but significant differences in transduction, implicating post-entry processing as the cause of divergent transduction. In the case of rAAV6 and rAAV1, differences in uptake more closely correlated with transduction differences, suggesting that receptor entry pathways likely play a more significant role in their divergent transduction biology of HAE. Thus, further investigation into the receptors utilized by AAV6 and AAV1 may lead to rational improvements in vector design for gene therapy to the airway.

MATERIALS AND METHODS

Recombinant AAV Vector Production

AAV1 helper plasmid p5E18RXC1 harboring AAV2 rep and AAV1 cap genes was kindly provided by Dr. James Wilson (University of Pennsylvania). pRep6Cap6 is an ITR-deleted AAV6 genome plasmid clone and was a gift from Dr. David Russell (University of Washington). To generate a common packaging system, AAV6 divergent capsid sequences were cloned into the AAV1 packaging system. The AAV1 and AAV6 capsid genes share identical nucleotide sequence at the immediate N-terminus of VP1 and a unique EcoN I site is located in this region. The portion of the AAV6 capsid gene after the EcoNI site was retrieved from plasmid pRep6Cap6 by EcoNI and BamHI digestion and used to replace the corresponding EcoNI-BamHI fragment in p5E18RXC1. The resultant plasmid (pR2C6) is the AAV6 helper plasmid and was used for pseudotyping rAAV6 virus in this study. Both pR2C6 and p5E18RXC1 link the AAV2 rep gene to the AAV6 and AAV1 cap genes, respectively; both having identical sequences with the exception of the 6 divergent capsid amino acids. All the other helper plasmids for the AAV6 mutants were constructed based on the pR2C6. The helpers for pR2C6-L584F, pR2C6-V598A and pR2C6-H642N were generated by site-directed mutagenesis with the Quick Change II kit from Stratagene. Helper plasmid pR2C6-F129L was generated by swapping the 603 bp EcoNI-KasI fragment from p5E18RXC1 into pR2C6. Helper plasmid pR2C6-D418E/K531E was generated by swapping the KasI to MscI 1068 bp fragment from p5E18RXC1 into pR2C6, whereas helper plasmid pR2C6-F129L/L584F/V598A/H642N was generated by swapping the same fragment from pR2C6 to p5E18RXC1. All the helper plasmids were sequence confirmed.

Viral stocks of rAAV packaged an identical AAV2 genome harboring a CMV-luciferase expression cassette and were generated by triple plasmids co-transfection using an adenovirus-free system as previously described[23]; this system uses the rAAV helper plasmid pAD Helper 4.1 (adenovirus helper plasmid) and pAV2-CMVLuc-flag (rAAV2 proviral plasmid). All rAAV1, rAAV6 and mutant viruses were purified with an identical procedure by two rounds of CsCl ultracentrifugation followed by ultracentrifugation sedimentation through two sucrose cushions of 30% and 50% (W/V). The virus pellet was then resuspended in PBS. The titers of viral preparations as DNase-resistant particles (DRP) were determined by TaqMan real time quantification PCR and confirmed with slot blot assays using a P^{32} labeled probe against luciferase gene. The purities of these vectors were analyzed in SDS-PAGE. No significant impurity protein bands were observed by Coomassie blue staining. The viruses were also examined by transmission electronic microscopy with negative staining. There were no obvious differences in virion aggregation and empty particles (without DNA packaged) were only infrequently observed for both serotypes.

Cell Culture and Virus Infection Conditions

293, HeLa, and IB3 cells were cultured as monolayers in Dulbecco's modified Eagle medium (DMEM), supplemented with 10% fetal bovine serum and penicillin-streptomycin, and maintained in a 37°C incubator at 5% CO_2. AAV infections were performed by directly adding the viruses at a MOI of 5000 DRP/cell to cell cultures in 24-well or 48-well plates at ~70% confluency. Viruses were left in the culture medium over the 24h infection period.

Polarized human airway epithelia were generated as previously described from lung transplant airway tissue[42] and were obtained from the Tissue and Cell Culture Core of The Center for Gene Therapy at the University of Iowa. Epithelia were grown on 12 mm Millicell membrane inserts (Millipore) and differentiated with USG medium at an air-liquid interface prior to use [42]. To apically infect the polarized airway epithelia, 5×10^9 DRP of rAAV were diluted in USG medium to the final volume of 50 μl and applied to the upper chamber of the Millicell insert. For basolateral infections, 5×10^9 DRP of rAAV containing medium was directly added to the culture medium in the bottom chamber. Viruses were exposed to epithelia for 16 hrs and then removed. At this time, the Millicell inserts were briefly washed with a small amount USG medium and fed with fresh USG medium to the bottom chamber only. Approximately 10^6 cells are in each Millicell insert and thus the multiplicity of infection (MOI) was ~5000 DRP/cell. Transduction was assessed by luciferase reporter assays at various time points post-infection using cell lysates or IVIS biophotonic imaging.

Measurement of luciferase reporter expression

Luciferase enzyme activity in cell lysates was determined using the Luciferase Assay System (Promega) in a 20/20 luminometer equipped with an automatic injector (Turner Biosystems). Quantification of luciferase activity in live cells was performed using the IVIS Biophotonic Imaging system according to the manufacturer's instructions. Images were taken 15 min after adding the VivoGlo Luciferin substrate (Promega) to the basolateral culture medium only and quantification of images were processed with the Living Image 2.51 software (Xenogen).

Analysis of internalized viral genome assay

Fully differentiated human polarized airway epithelia were infected with 5×10^9 particles of rAAV. After a 4 hr infection period, virus was removed by extensive washing with PBS. The Millicell inserts then were fed with fresh medium in the bottom chamber and put back to 37°C incubator until 18 hr or 3 day post-infection time points. At these two time-points, each Millicell insert was washed thoroughly with 40 ml PBS in a 50 ml conical tube three times, then the cells were lysed with 100 μl luciferase cell lysis buffer for both luciferase assays and PCR quantification of viral genomes. For PCR analysis, 10 μl of this cell lysate was mixed with 40 μl digestion buffer (50 mM KCl, 2.5 mM MgCl, 10 mM Tris pH 8.0, 0.5% NP40, 0.5% Tween-20 and 400 μg/ml proteinase K). After digestion at 56°C for 45 min and heat-inactivation at 95°C for 15 min, 1 μl of the digestion was used for TaqMan PCR. Viral genome assays on HeLa and IB3 cells were similarly performed, except the cells were trypsinized and the cell pellets were washed twice before the proteinase K digestion in 50 μl of the above digestion buffer.

Quantitative analysis of rAAV genome by TaqMan PCR

TaqMan real time PCR was used to quantify the physical titer of the viral stocks and copies of viral genome in cell lysates from AAV infected cells as previously described[23, 32]. The PCR primers used were 5′-TTTTTGAAGCGAAGGTTGTGG-3′ (forward) and 5′-CACACACA GTTCGCCTCTTTG-3′ (reverse) and amplify a 73 bp fragment of the rAAV2.Luc genome. The Taqman probe (5′-

ATCTGGATACCGGGAAAACGCTGGGCGTTAAT-3′) was synthesized by IDT (Coralville, IA). This probe was tagged with 6-carboxy fluorescein (FAM) at the 5′-end as the reporter and Dark Hole Quencher 1 (BHQ1) at the 3′-end as the quencher. The PCR reaction was performed and analyzed using Bio-Rad MyIQ™ Real-time PCR detection system and software.

Statistics analysis

Data are expressed as means +/− SEM of n independent observations. Data analyses were conducted using the nonparametric Mann-Whitney test for comparison of two data sets or One-way ANOVA with a Tukey's post-test for comparison of three or more data sets. All statistical analysis used Prism software. In all statistical analyses, p values <0.05 were deemed significant.

Acknowledgments

This work was supported by NIH grants HL108902 (to JFE), the Roy J. Carver Chair in Molecular Medicine (to JFE), and the University of Iowa Center for Gene Therapy (DK54759).

References

1. Blacklow, NR. Adeno-associated viruses of human. In: Pattison, JR., editor. Parvoviruses and Human Disease. CRC Press; Boca Raton: 1988. p. 165-174.
2. Carter BJ. Adeno-associated virus and the development of adeno-associated virus vectors: a historical perspective. Mol Ther. 2004; 10(6):981–9. [PubMed: 15564130]
3. Carter BJ. Adeno-associated virus vectors in clinical trials. Hum Gene Ther. 2005; 16(5):541–50. [PubMed: 15916479]
4. Gao G, Vandenberghe LH, Wilson JM. New recombinant serotypes of AAV vectors. Curr Gene Ther. 2005; 5(3):285–97. [PubMed: 15975006]
5. Wu Z, Asokan A, Samulski RJ. Adeno-associated virus serotypes: vector toolkit for human gene therapy. Mol Ther. 2006; 14(3):316–27. [PubMed: 16824801]
6. Zincarelli C, Soltys S, Rengo G, Rabinowitz JE. Analysis of AAV serotypes 1–9 mediated gene expression and tropism in mice after systemic injection. Mol Ther. 2008; 16(6):1073–80. [PubMed: 18414476]
7. Schaffer DV, Maheshri N. Directed evolution of AAV mutants for enhanced gene delivery. Conf Proc IEEE Eng Med Biol Soc. 2004; 5:3520–3. [PubMed: 17271049]
8. Koerber JT, Jang JH, Schaffer DV. DNA shuffling of adeno-associated virus yields functionally diverse viral progeny. Mol Ther. 2008; 16(10):1703–9. [PubMed: 18728640]
9. Excoffon KJ, Koerber JT, Dickey DD, Murtha M, Keshavjee S, Kaspar BK, et al. Directed evolution of adeno-associated virus to an infectious respiratory virus. Proc Natl Acad Sci U S A. 2009; 106(10):3865–70. [PubMed: 19237554]
10. Boutin S, Monteilhet V, Veron P, Leborgne C, Benveniste O, Montus MF, et al. Prevalence of serum IgG and neutralizing factors against adeno-associated virus (AAV) types 1, 2, 5, 6, 8, and 9 in the healthy population: implications for gene therapy using AAV vectors. Hum Gene Ther. 2010; 21(6):704–12. [PubMed: 20095819]
11. Padron E, Bowman V, Kaludov N, Govindasamy L, Levy H, Nick P, et al. Structure of adeno-associated virus type 4. J Virol. 2005; 79(8):5047–58. [PubMed: 15795290]
12. Li W, Zhang L, Johnson JS, Zhijian W, Grieger JC, Ping-Jie X, et al. Generation of novel AAV variants by directed evolution for improved CFTR delivery to human ciliated airway epithelium. Mol Ther. 2009; 17(12):2067–77. [PubMed: 19603002]

13. Halbert CL, Allen JM, Miller AD. Adeno-associated virus type 6 (AAV6) vectors mediate efficient transduction of airway epithelial cells in mouse lungs compared to that of AAV2 vectors. J Virol. 2001; 75(14):6615–24. [PubMed: 11413329]
14. Wu Z, Asokan A, Grieger JC, Govindasamy L, Agbandje-McKenna M, Samulski RJ. Single amino acid changes can influence titer, heparin binding, and tissue tropism in different adeno-associated virus serotypes. J Virol. 2006; 80(22):11393–7. [PubMed: 16943302]
15. Wu Z, Miller E, Agbandje-McKenna M, Samulski RJ. Alpha2,3 and alpha2,6 N-linked sialic acids facilitate efficient binding and transduction by adeno-associated virus types 1 and 6. J Virol. 2006; 80(18):9093–103. [PubMed: 16940521]
16. Grimm D, Zhou S, Nakai H, Thomas CE, Storm TA, Fuess S, et al. Preclinical in vivo evaluation of pseudotyped adeno-associated virus vectors for liver gene therapy. Blood. 2003; 102(7):2412–9. [PubMed: 12791653]
17. Grimm D, Kay MA, Kleinschmidt JA. Helper virus-free, optically controllable, and two-plasmid-based production of adeno-associated virus vectors of serotypes 1 to 6. Mol Ther. 2003; 7(6):839–50. [PubMed: 12788658]
18. Flotte TR. Recent developments in recombinant AAV-mediated gene therapy for lung diseases. Curr Gene Ther. 2005; 5(3):361–6. [PubMed: 15975013]
19. Aitken ML, Moss RB, Waltz DA, Dovey ME, Tonelli MR, McNamara SC, et al. A phase I study of aerosolized administration of tgAAVCF to cystic fibrosis subjects with mild lung disease. Hum Gene Ther. 2001; 12(15):1907–16. [PubMed: 11589832]
20. Wagner JA, Nepomuceno IB, Messner AH, Moran ML, Batson EP, Dimiceli S, et al. A phase II, double-blind, randomized, placebo-controlled clinical trial of tgAAVCF using maxillary sinus delivery in patients with cystic fibrosis with antrostomies. Hum Gene Ther. 2002; 13(11):1349–59. [PubMed: 12162817]
21. Moss RB, Milla C, Colombo J, Accurso F, Zeitlin PL, Clancy JP, et al. Repeated aerosolized AAV-CFTR for treatment of cystic fibrosis: a randomized placebo-controlled phase 2B trial. Hum Gene Ther. 2007; 18(8):726–32. [PubMed: 17685853]
22. Duan D, Yue Y, Yan Z, Yang J, Engelhardt JF. Endosomal processing limits gene transfer to polarized airway epithelia by adeno-associated virus. J Clin Invest. 2000; 105(11):1573–87. [PubMed: 10841516]
23. Yan Z, Lei-Butters DC, Liu X, Zhang Y, Zhang L, Luo M, et al. Unique biologic properties of recombinant AAV1 transduction in polarized human airway epithelia. J Biol Chem. 2006; 281(40):29684–92. [PubMed: 16899463]
24. Yan Z, Zak R, Luxton GW, Ritchie TC, Bantel-Schaal U, Engelhardt JF. Ubiquitination of both adeno-associated virus type 2 and 5 capsid proteins affects the transduction efficiency of recombinant vectors. J Virol. 2002; 76(5):2043–53. [PubMed: 11836382]
25. Zhong L, Li B, Jayandharan G, Mah CS, Govindasamy L, Agbandje-McKenna M, et al. Tyrosine-phosphorylation of AAV2 vectors and its consequences on viral intracellular trafficking and transgene expression. Virology. 2008; 381(2):194–202. [PubMed: 18834608]
26. Zhong L, Li B, Mah CS, Govindasamy L, Agbandje-McKenna M, Cooper M, et al. Next generation of adeno-associated virus 2 vectors: point mutations in tyrosines lead to high-efficiency transduction at lower doses. Proc Natl Acad Sci U S A. 2008; 105(22):7827–32. [PubMed: 18511559]
27. Ding W, Zhang L, Yan Z, Engelhardt JF. Intracellular trafficking of adeno-associated viral vectors. Gene Ther. 2005; 12(11):873–80. [PubMed: 15829993]
28. Limberis MP, Vandenberghe LH, Zhang L, Pickles RJ, Wilson JM. Transduction efficiencies of novel AAV vectors in mouse airway epithelium in vivo and human ciliated airway epithelium in vitro. Mol Ther. 2009; 17(2):294–301. [PubMed: 19066597]
29. Virella-Lowell I, Zusman B, Foust K, Loiler S, Conlon T, Song S, et al. Enhancing rAAV vector expression in the lung. J Gene Med. 2005; 7(7):842–50. [PubMed: 15838934]
30. Halbert CL, Madtes DK, Vaughan AE, Wang Z, Storb R, Tapscott SJ, et al. Expression of human alpha1-antitrypsin in mice and dogs following AAV6 vector-mediated gene transfer to the lungs. Mol Ther. 2010; 18(6):1165–72. [PubMed: 20372105]

31. Flotte TR, Fischer AC, Goetzmann J, Mueller C, Cebotaru L, Yan Z, et al. Dual reporter comparative indexing of rAAV pseudotyped vectors in chimpanzee airway. Mol Ther. 2010; 18 (3):594–600. [PubMed: 19826405]
32. Ding W, Zhang LN, Yeaman C, Engelhardt JF. rAAV2 traffics through both the late and the recycling endosomes in a dose-dependent fashion. Mol Ther. 2006; 13(4):671–82. [PubMed: 16442847]
33. Agbandje-McKenna M, Kleinschmidt J. AAV capsid structure and cell interactions. Methods Mol Biol. 2011; 807:47–92. [PubMed: 22034026]
34. Chapman, MS.; Agbandje-McKenna, M. Atomic structure of viral particles. In: KJ, R.; CS, F.; BM, E.; LR, M.; PC, R., editors. Parvoviruses. Edward Arnold, Ltd; New York, NY: 2006. p. 107-123.
35. Ng R, Govindasamy L, Gurda BL, McKenna R, Kozyreva OG, Samulski RJ, et al. Structural characterization of the dual glycan binding adeno-associated virus serotype 6. J Virol. 2010; 84 (24):12945–57. [PubMed: 20861247]
36. Nam HJ, Gurda BL, McKenna R, Potter M, Byrne B, Salganik M, et al. Structural studies of adeno-associated virus serotype 8 capsid transitions associated with endosomal trafficking. J Virol. 2011; 85(22):11791–9. [PubMed: 21900159]
37. Lerch TF, Xie Q, Chapman MS. The structure of adeno-associated virus serotype 3B (AAV-3B): insights into receptor binding and immune evasion. Virology. 2010; 403(1):26–36. [PubMed: 20444480]
38. Liu X, Luo M, Guo C, Yan Z, Wang Y, Engelhardt JF. Comparative biology of rAAV transduction in ferret, pig and human airway epithelia. Gene Ther. 2007; 14(21):1543–8. [PubMed: 17728794]
39. Liu X, Luo M, Trygg C, Yan Z, Lei-Butters DC, Smith CI, et al. Biological Differences in rAAV Transduction of Airway Epithelia in Humans and in Old World Non-human Primates. Mol Ther. 2007; 15(12):2114–23. [PubMed: 17667945]
40. Liu X, Yan Z, Luo M, Engelhardt JF. Species-specific differences in mouse and human airway epithelial biology of recombinant adeno-associated virus transduction. Am J Respir Cell Mol Biol. 2006; 34(1):56–64. [PubMed: 16195538]
41. Li W, Zhang L, Wu Z, Pickles RJ, Samulski RJ. AAV-6 mediated efficient transduction of mouse lower airways. Virology. 2011; 417(2):327–33. [PubMed: 21752418]
42. Karp PH, Moninger TO, Weber SP, Nesselhauf TS, Launspach JL, Zabner J, et al. An in vitro model of differentiated human airway epithelia. Methods for establishing primary cultures. Methods Mol Biol. 2002; 188:115–37. [PubMed: 11987537]

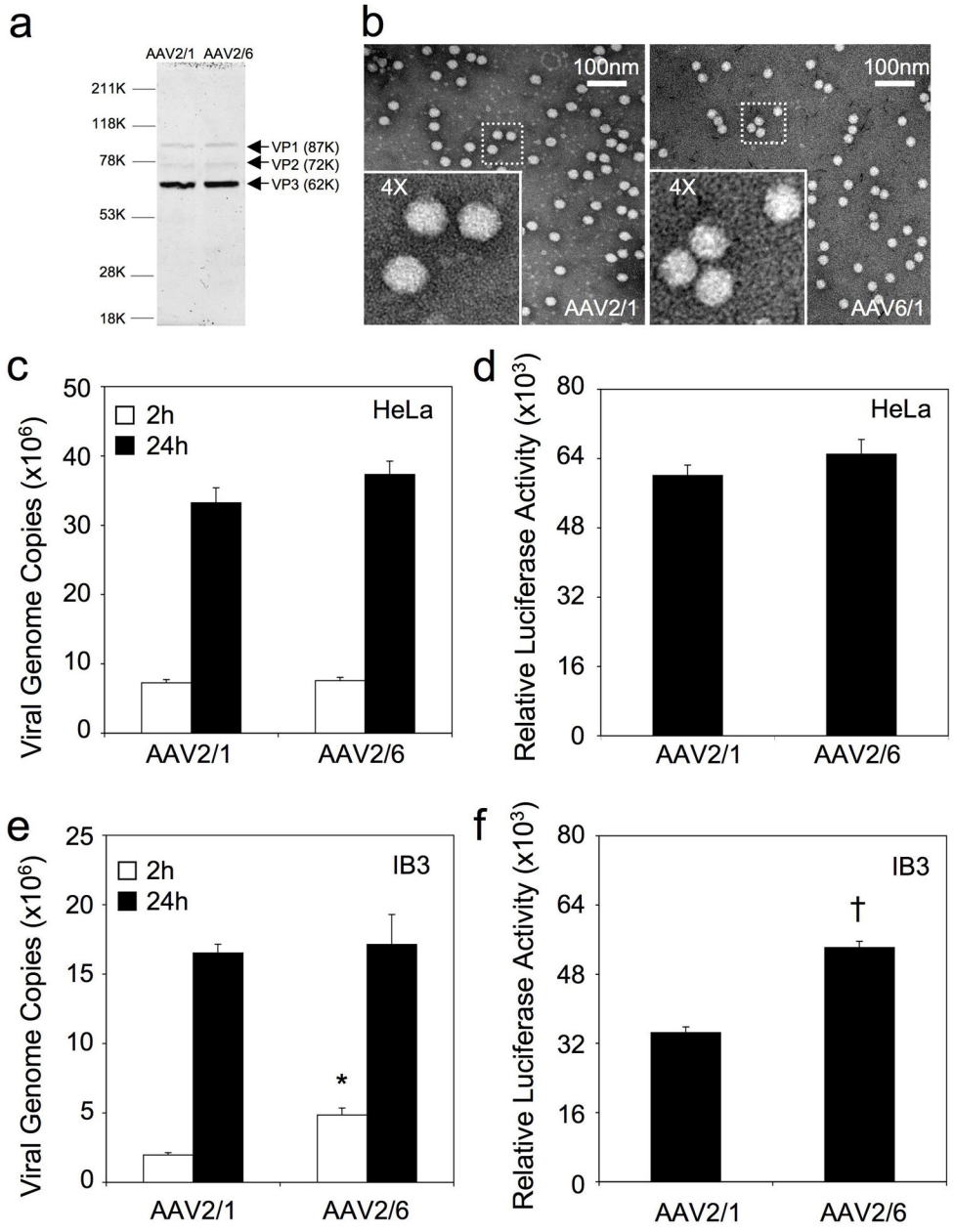

Figure 1.

Quality control analysis of rAAV2/1 and rAAV2/6 viral preparation on cell lines. (a) rAAV2/1 and rAAV2/6 were purified by CsCl banding followed by sucrose cushion ultracentrifugation. Viral stocks were then examined by SDS-PAGE followed by Coomassie Blue staining (4×10^9 DRP per lane). The three major AAV capsid proteins VP1, 2, and 3 are marked by arrows. (b) Negatively-stained transmission electron micrographs reveal no virion aggregations and few empty virions for both serotypes. (c– f) Functional analysis of rAAV2/1.Luc and rAAV2/6.Luc infection in HeLa and IB3 cells. Viral genome uptake by cells at 2 and 24 hrs post-infection was quantified by TaqMan PCR in (c) HeLa cells and (e) IB3 cells. Infections were performed at ~70% confluence in 24-well plates at a multiplicity

of infection (MOI) of 5000 DRP per cell. Data represents the mean (+/− SEM) viral genome copies (per well) from 3–4 independent experiments (n is indicated in the graph). Luciferase expression from rAAV2/1.Luc and rAAV2/6.Luc-infected (d) HeLa cells and (f) IB3 cells was measured at 24 hrs post-infection. Infections were performed under the same conditions for genome analysis (MOI = 5000 DRP per cell). Data represents the mean (+/− SEM) relative luciferase activity (per well) from six independent experiments (n=6). Statistical analyses using the nonparametric Mann-Whitney test demonstrated significance for only 2h viral DNA uptake (*, $p<0.005$) and 24h transgene expression (†, $p<0.005$) between rAAV2/1 and rAAV2/6 infections in IB3 cells.

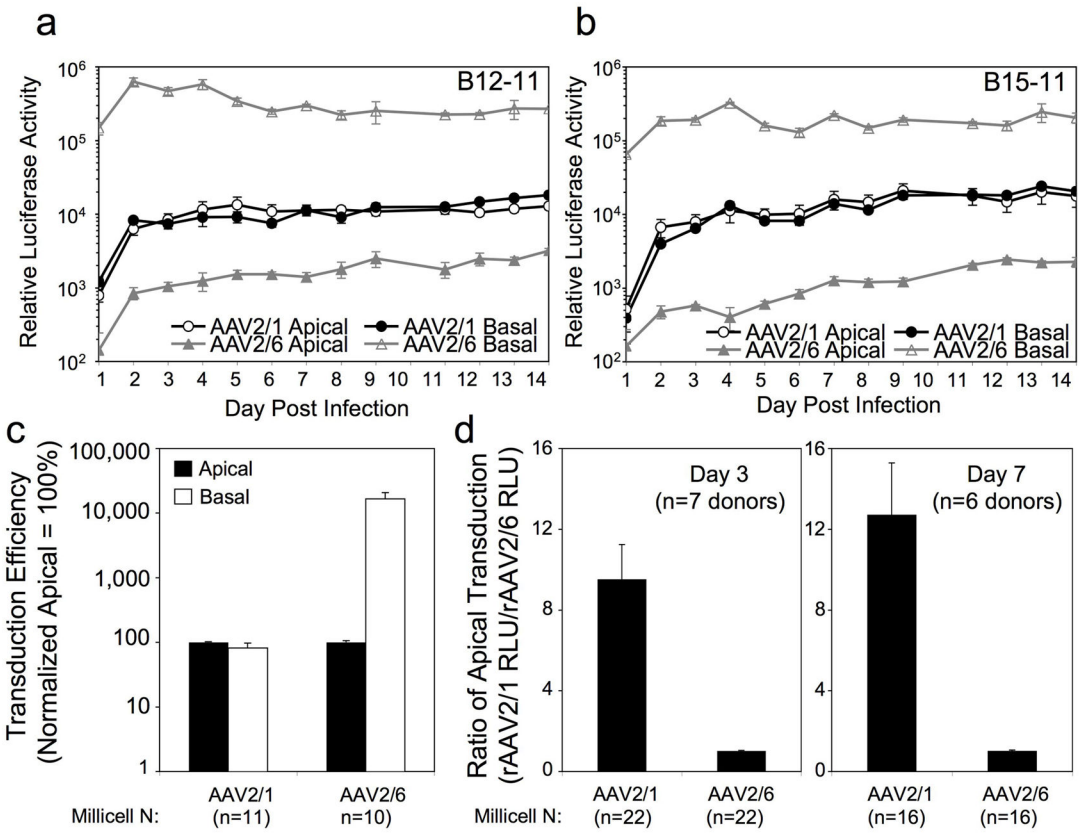

Figure 2.

Transduction profiles of rAAV2/1 and rAAV2/6 on polarized human airway epithelia following apical and basolateral infection. (a, b) Time-course comparison of rAAV2/1- and rAAV2/6-mediated luciferase expressions using two independent human airway donors (B12-11 and B15-11). 5×10^9 DRP of AAV2/1.Luc or AAV2/6.Luc were applied to either the apical or the basolateral surface of polarized airway epithelia (n=3 Millicell inserts per infection condition). Luciferase expression was monitored over 14 days by biophotonic imaging of live cells using the Xenogen 200 IVIS. Lucigenin substrate was added to the culture medium 15 min before the measurements were taken. Data represents the mean (+/− SEM) relative luciferase activity per well (n=3 independent wells). (c) Comparison of the transduction polarity of rAAV2/1 and rAAV2/6 at 3 days following apical and basolateral infection. The infection conditions were the same is (a). Data represents the mean (+/− SEM) transduction efficiency normalized to apical as 100% for each of the 8 independent donor samples tested (n=11 independent rAAV2/1 infections with four different viral preparation and n=10 independent rAAV1/6 infections with three different viral preparation). The raw data used to generate this graph is summarized in Table 1 for each individual donor sample tested. Statistical analyses using the nonparametric Mann-Whitney test demonstrated the difference between the apical and basolateral infections were significant for rAAV2/6 ($p<0.0001$) but not for rAAV2/1. (d) Comparison of the apical transduction efficiencies of rAAV2/1 and rAAV2/6 at 3 and 7 days post-infection. As summarized in Table 2, the ratio of rAAV2/1 apical transduction divided by rAAV2/6 apical transduction were calculated at 3 and 7 days post-infection for each donor sample tested.

Value represents the mean (+/− SEM) at 3 days post-infection (n=7 independent donors samples) and 7 days post-infection (n=6 independent donors samples). Statistical analyses using the nonparametric Mann-Whitney test demonstrated that the differences between rAAV2/2 and rAAV2/6 were significant (3 day, $p<0.001$; 7 day $p<0.005$).

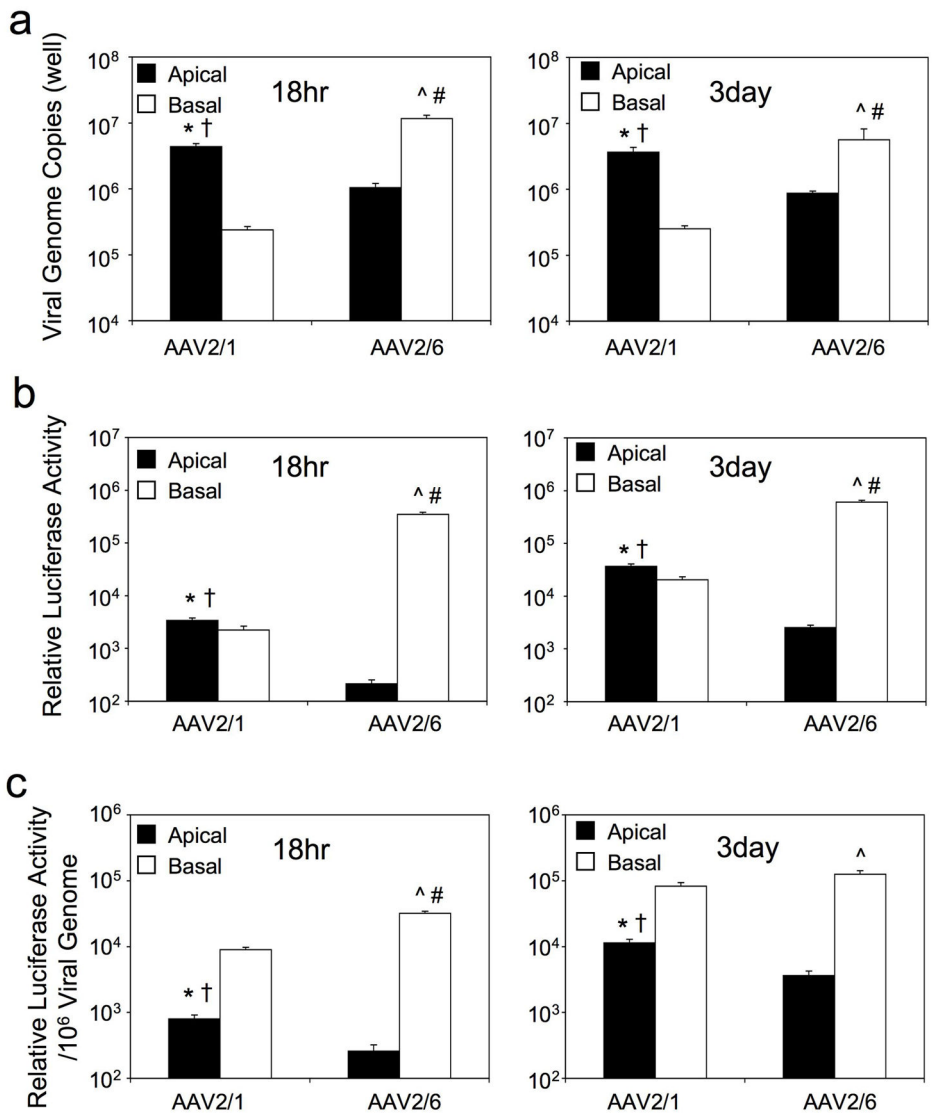

Figure 3.

Comparison of viral uptake and transduction following infection of polarized human airway epithelia with rAAV2/1 and rAAV2/6. Polarized human airway epithelia were infected with 5×10^9 DRP of rAAV2/1 or rAAV2/6 from either apical or basolateral membranes. Cultures were washed thoroughly at 4 hour post-infection to remove extracellular virus and infections were continued until the 18 hrs and 3 days time points. The cells were then lysed, and (a) internalized viral genomes were quantified by TaqMan PCR and (b) luciferase activity was determined on the cell lysates. (c) rAAV2/1 and rAAV2/6 vector efficiencies were calculated as transgene expression per viral genome. Data represents the mean (+/− SEM) values from n=7 independent infections at each of the time points. Statistical analysis was performed using the nonparametric Mann-Whitney test. Significant differences ($p<0.05$) between the comparisons were marked as follows: * rAAV2/1 apical infection vs. rAAV2/1 basolateral infection, † rAAV2/1 apical infection vs. rAAV2/6 apical infection, ^ rAAV2/6

apical infection vs. rAAV2/6 basolateral infection, # rAAV2/6 basolateral infection vs. rAAV2/1 basolateral infection.

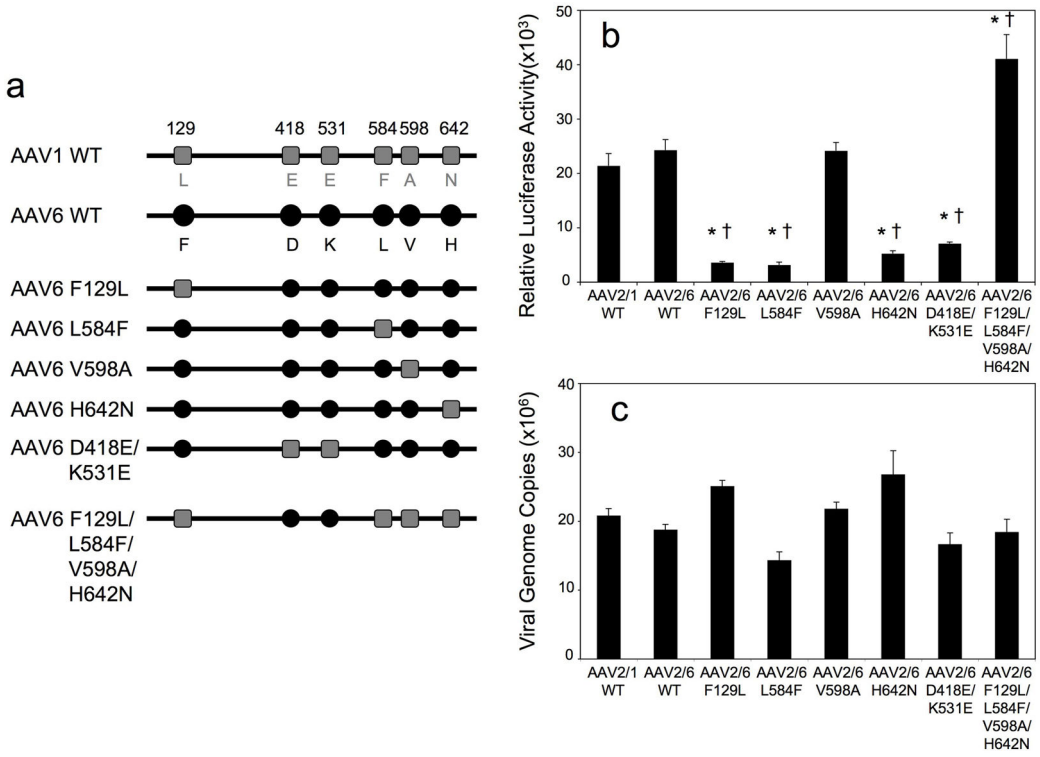

Figure 4.

rAAV2/6 mutant vectors and their transduction profiles in HeLa cells. (a) Schematic representation of the amino acid differences in the capsid of wild type AAV1, AAV6 and the six AAV mutants generated by introducing AAV1 amino acid residues into the AAV6 capsids. The six amino acid residues that vary between AAV1 and AAV6 capsids are marked with grey squares for the AAV1 sequence and black circles for AAV6 sequence. (b) Transduction profiles of luciferase-expressing rAAV1-WT, rAAV6-WT, and the various mutant viruses in HeLa cells. MOI was equal to 5000 DRP/cell for all the infections and luciferase activities in cell lysates were measured at 24 hr post-infection. Data represents the mean (+/− SEM) relative luciferase activity (per well) for n=4 independent experiments. Statistical analysis was performed using one-way ANOVA with Tukey's multiple comparison post-test (*$p<0.001$, rAAV2/1-WT vs. mutants; †$p<0.001$, rAAV2/6-WT vs. mutants). (c) TaqMan PCR was used to quantify internalized viral genome at 24 hrs following infection of HeLa cells with rAAV1-WT, rAAV6-WT, and the various mutants. Data represents the mean (+/− SEM) viral genome copies (per well) for n=4 independent experiments.

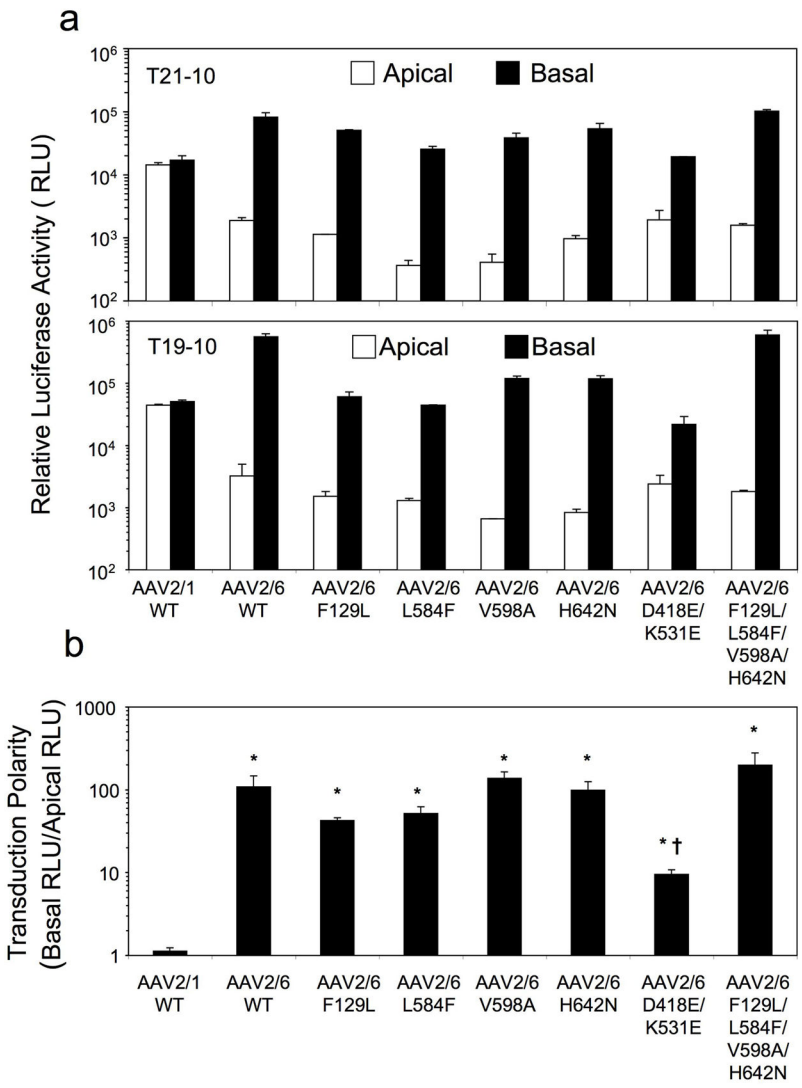

Figure 5.

Comparison of the transduction profiles of rAAV1-WT, rAAV6-WT, and the various mutants following apical or basolateral infection of polarized human airway epithelia. Human polarized airway epithelial cultures were infected with 5×10^9 DRP/well of AAV2/1.Luc, AAV2/6.Luc and the various mutant vectors from either the apical or basolateral surface of polarized airway epithelial cultures. Duplicate infections were performed for each infection condition on cells from two independent donors (T21-10 and B19-10). (a) Luciferase expressions at 7 days following apical or basolateral infections with the various vectors. Data represents the mean (+/− range) relative luciferase activity. (b) Transduction polarity was calculated as the ratio of luciferase activity seen following basolateral infection divided by that observed following apical infection. Data represents the mean (+/− SEM) transduction polarity ratio for n=4 paired infections from two donor samples. Statistical analysis was performed using one-way ANOVA with Tukey's multiple comparison post-test (*$p<0.05$, rAAV2/1-WT vs. rAAV2/6-WT and mutants; †$p<0.05$,

rAAV2/6-WT vs mutants, only rAAV2/6-D418E/K531E demonstrated a significant difference in comparison to rAAV2/6-WT).

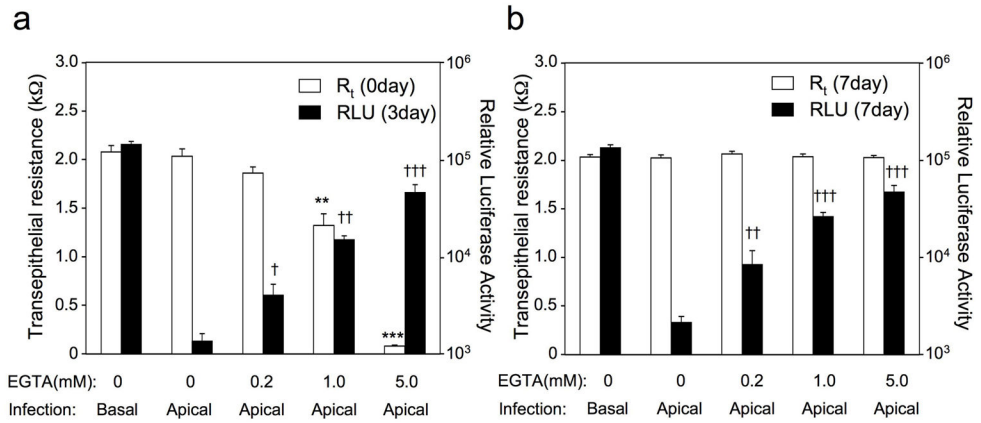

Figure 6.

Changes in resistance of human airway epithelia influence rAAV2/6 transduction with virus applied to the apical surface. Various degrees of transient tight junction disruption were induced at the time of infection by adding 200 μl of PBS containing the indicated concentration of EGTA to the apical chamber for 5 min. The EGTA solution was then removed and epithelia were washed twice with USG medium. During the period of the last wash, the transepithelial resistance (R_t) was measured with an ohmmeter. After measuring R_t and removing all the media from the apical chamber, the epithelia were infected with 5×10^9 DRP of rAAV2/6.Luc from the apical surface. Vehicle controls (0 mM EGTA) were treated identically with solutions lacking EGTA and infected with the same dose of rAAV2/6.Luc from the apical or basal membrane. Luciferase expression on 3 and 7 days post-infection were measured by imaging of live cells using the Xenogen 200 IVIS. The R_t of each MilliCell was also measured 7 days after luciferase imaging to confirm restoration of normal polarity. (a) The average R_t of epithelia prior to infection and the relative luciferase activity at 3 days post-infection. (b) The average R_t of epithelia and relative luciferase activity at 7 days post-infection. Data represents the mean (+/− SEM) relative luciferase activity (RLU/per well) and the transepithelial resistance (R_t) of each test group (n=7). Statistical analysis was performed using the nonparametric Mann-Whitney test (**p<0.005 and ***p<0.001, R_t of EGTA-treated cells vs. mock-treated cells; †p<0.05, ††p<0.005, and †††p<0.001, apical transgene expression of EGTA-treated cells vs. mock-treated cells).

Table 1

Transduction polarity indexes of rAAV2/1 and rAAV2/6 vectors following infection of human polarized airway epithelia from multiple donors.

	Donor Tissue Sample							
Serotype (Viral Prep)	**B23-09 (n=3)**	**B10-10 (n=6)**	**B16-10 (n=3)**	**T21-10 (n=2)**	**B19-10 (n=2)**	**B31-10 (n=3)**	**B12-11 (n=3)**	**B15-11 (n=3)**
rAAV2/1 (Lot#:121309)	0.22 +/−0.01							
rAAV2/1 (Lot#:022610)	0.38 +/−0.07							
rAAV2/1 (Lot#:071010)		2.19 +/−0.51	0.92 +/−0.16	0.55 +/−0.09	1.05 +/−0.30	0.31 +/−0.08	0.87 +/−0.12	0.81 +/−0.02
rAAV2/1 (Lot#:110710)				0.65 +/0.03	1.00 +/−0.05			
rAAV2/6 (Lot#:022610)	68.00 +/−8.4			85.48 +/−14.91				
rAAV2/6 (Lot#:071010)		70.59 +/9.47	145.11 +/−10.33	54.04 +/−8.13	220.32 +/−3.51	185.06 +/8.04	445.66 +/−30.67	330.10 +/−13.17
rAAV2/6 (Lot#:110710)				53.35 +/−8.94				

Value represents the ratio of rAAV basolateral transduction divided by apical transduction at 3-day post-infection for each serotype and donor epithelia evaluated [+/− SEM (N ≥ 3) or +/− range (n=2)].

Table 2

Comparison of rAAV2/1 apical transduction efficiency to rAAV2/6

	Donor Tissue Sample						
Time Post-Infection	**B10-10 (n=6)**	**B16-10 (n=3)**	**T21-10 (n=2)**	**B19-10 (n=2)**	**B31-10 (n=3)**	**B12-11 (n=3)**	**B15-11 (n=3)**
Day3	11.22 +/−2.53	5.45 +/−0.57	3.73 +/−0.27	7.45 +/−0.53	16.73 +/−1.54	8.07 +/1.53	13.72 +/−3.42
Day7	ND	21.14 +/−3.47	2.31 +/−0.12	14.50 +/−1.75	13.20 +/−3.32	9.47 +/−1.06	15.53 +/−4.48

Value represents the ratio of rAAV2/1 apical transduction divided by rAAV2/6 apical transduction at 3 and 7 day post-infection time points [+/− SEM (N ≥ 3) or +/− range (n=2)].